Pharmacogn. Mag.
A multifaceted peer reviewed journal in the field of Pharmacognosy and Natural Products
www.phcog.com | www.phcog.net

ORIGINAL ARTICLE

Abyssomicin W and Neoabyssomicin B are Potential Inhibitors of New Delhi Metallo-β-Lactamase-1 (NDM -1): A Computational Approach

Abdulrahman Alsultan, Mohammad Aatif[1], Ghazala Muteeb[2]

Department of Biomedical Sciences, College of Medicine, Departments of [1]Public Health and [2]Nursing, College of Applied Medical Science, King Faisal University, Al-Ahsa 31982, Saudi Arabia

Submitted: 30-Apr-2022 Revised: 02-Jul-2022 Accepted: 15-Sep-2022 Published: 04-Nov-2022

ABSTRACT

Background: Antibiotic resistance in bacteria mediated by New Delhi Metallo-β-lactamase (NDM) is a global threat to human health with an enormous economic burden. NDM can hydrolyze all the β-lactam core-containing antibiotics including carbapenems, which are regarded as last resort antibiotics. **Materials and Methods:** A library of Abyssomicins was virtually screened to identify novel non-β-lactam ring-containing inhibitors of NDM-1. Different computational approaches such as molecular modeling, virtual screening, molecular docking, molecular dynamics simulation, ADMET profiling, and free energy calculations were utilized for this purpose. **Results:** Virtual screening and ADMET profiling shortlisted Abyssomicin W and Neoabyssomicin B as the most promising candidate molecules. An in-depth analysis of protein-ligand interactions by molecular docking revealed that both ligands bind the active site of NDM-1. The identified inhibitors interacted with key catalytic residues as well as other residues around the active site of NDM-1. Hydrogen bonding and hydrophobic interactions played a significant role in stabilizing the protein-inhibitor complexes. The docking energy of NDM-1-Abyssomicin W, and NDM-1-Neoabyssomicin B complexes were – 9.6 kcal/mol and – 9.5 kcal/mol, respectively, which were higher than NDM-1-Methicillin (control) complex (–7.3 kcal/mol). Molecular dynamics simulation and free energy calculations by MM-PBSA also confirmed the stability of NDM-1-Abyssomicin W, and NDM-1-Neoabyssomicin B complexes. **Conclusion:** The findings of this study suggest that Abyssomicins serve as potential inhibitors of NDM-1. However, these results need to be validated *in vitro* and *in vivo*. This study may serve as a basis for further developing Abyssomicins as novel inhibitors of β-lactamases.

Key words: Antibiotic resistance, molecular docking and simulation, multidrug resistance, natural compounds, structure-based drug design

SUMMARY

- The findings of this study suggest the possible use of Abyssomicin W and Neoabyssomicin B as a scaffold for the development of more potent inhibitors of NDM-1 which may serve as a novel therapeutic intervention in addressing antibiotic resistance problem.

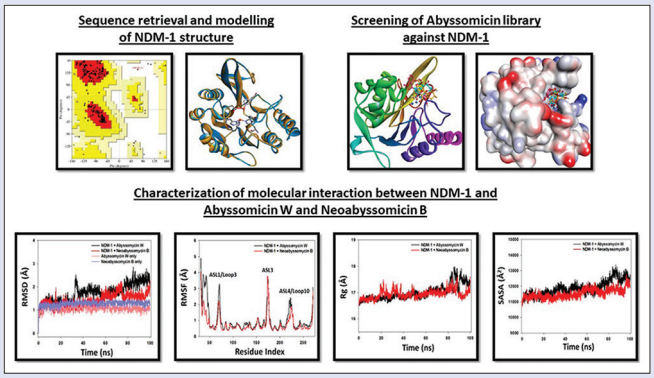

Abbreviations used: NDM-1: New Delhi Metallo-β-lactamase-1; ADMET: Absorption, Distribution, Metabolism, Excretion and Toxicity; MM-PBSA Molecular Mechanics-Poisson Boltzmann Surface Area ; MDR: Multi Drug Resistance ; CDC: Centers for Disease Control and Prevention; MRSA: Multidrug-Resistant *Staphylococcus aureus*; VRE: Vancomycin Resistant Enterococci; MBL: Metallo-β-lactamases; ESBLs: Extended-Spectrum Cephalosporinase; Paba: p-aminobenzoic acid ; ADCS: 4-amino-4-deoxychorismate synthase; PSVS: Protein Structure Validation Suite; ADT: AutoDock tools ; UFF: Universal Force Field ; LGA: Lamarck Genetic Algorithm

Correspondence:

Dr. Ghazala Muteeb,
Department of Nursing, College of Applied Medical Science, King Faisal University, Al-Ahsa 31982, Saudi Arabia.
E-mail: graza@kfu.edu.sa
DOI: 10.4103/pm.pm_195_22

Access this article online
Website: www.phcog.com
Quick Response Code:

INTRODUCTION

Antibiotic resistance is an emerging global threat with a huge social and economic impact. Bacteria develop resistance to antibiotics due to their overuse and misuse, thereby endangering the potential of antibiotics.[1-3] The problem is further augmented by the lack of new drugs in pharmaceutical pipelines pertaining to reduced profits and difficult drug regulatory rules.[4] Infections caused by antibiotic-resistant bacteria have been reported in different parts of the globe. Many health organizations have warned of the rapid emergence of antibiotic resistance as a "crisis" or "nightmare scenario" having "catastrophic consequences".[5] In 2012, CDC (Centers for Disease Control and Prevention) declared that the human race is facing a "post-antibiotic era", and WHO (World Health Organization) warned that the problem of antibiotic resistance is of dire consequences.[6] The phenomenon of multidrug resistance (MDR) in Gram-negative bacteria is observed not only in hospital settings (caused

Cite this article as: Alsultan A, Aatif M, Muteeb G. Abyssomicin W and neoabyssomicin B are potential inhibitors of New Delhi metallo-β-Lactamase-1 (NDM -1): A computational approach. Phcog Mag 2022;18:893-902.

by *Klebsiella pneumonia*, *Pseudomonas aeruginosa*, and *Acinetobacter baumanii*) but it has spread to a community setting (caused by *Escherichia coli* and *Neisseria gonorrhoeae*) as well.[7] MDR is also reported in Gram-positive bacteria such as *Staphylococcus aureus* and Enterococcus species causing MRSA (multidrug-resistant *Staphylococcus aureus*) and VRE (Vancomycin-resistant enterococci), respectively.[8]

The most prevalent mechanism of resistance in bacteria is the production of β-lactamases, which can hydrolyze β-lactam rings containing antibiotics. Other methods of antibiotic resistance development include modification of target enzyme, production of drug-efflux pumps, expression of drug-modifying enzymes, etc.[9,10] Ambler has classified β-lactamases into four classes namely A, B, C, and D.[11] The β-lactamases use either Serine residue (β-lactamases in classes A, C, and D) or metal ion (β-lactamases in class B, also known as Metallo-β-lactamases i.e. MBL) at the active site to hydrolyze β-lactam antibiotics. MBLs are further classified into sub-groups B1, B2, and B3, amongst which sub-group B1 is the most relevant clinically. Based on their functionality, Bush *et al.* (2010)[12] have classified β-lactamases into different groups such as group 1 containing Cephalosporinase; group 2 comprising Oxacillinase, Penicillinase, ESBLs (extended-spectrum cephalosporinase), and seine-based carbapenemase; and group 3 belonging to metal-based carbapenemase. The newly reported New Delhi Metallo-β-lactamases-1 (NDM-1) is an example of Ambler class B1 MBL, belonging to Bush's group 3 functionality.

The widespread dissemination of NDM-1 in clinical, as well as community settings, is a great threat to human beings owing to its ability to hydrolyze almost all types of β-lactam antibiotics like penicillins, cephalosporins, and carbapenems, except monobactams. In 2009, NDM-1 was reported for the first time in a Swedish patient getting medical treatment in India.[13] Since then, NDM-1 has been disseminated globally on all the continents and different countries such as the USA, UK, Canada, Australia, Austria, Belgium, Sweden, France, Germany, Japan, Netherland, China, Saudi Arabia, Oman, Pakistan, Bangladesh, Africa, etc.[14] Poirel *et al.* (2011)[15] have documented for the first time the spread of blaNDM-1 in the Arabian Peninsula and the Middle East. Also, the *Enterobacteriaceae* bacteria expressing blaNDM-1 have been reported in Kuwait and Lebanon.[16,17] Recently, 11 NDM-1, 5 OXA-48, and 1 NDM-1 + OXA-181 carbapenem-resistant bacterial isolates have been reported from Oman.[18] In Saudi Arabia, the recent emergence of NDM-1, OXA-48, and VIM in *Klebsiella pneumoniae*, suggests that multidrug-resistant carbapenemases are emerging in the region.

Abyssomicins are natural products belonging to the spirotetronate polyketide family of antibiotics which are mainly antimicrobial, antiviral, anticancer, anti-tuberculosis, etc.[19-21] In 2004, Abyssomicin C was isolated for the first time from actinomycete *Verrucosispora maris*.[22,23] Abyssocmycin C has been shown to possess promising activity against *Staphylococcus aureus* (MRSA), and tuberculosis causing mycobacteria.[24,25] It acts by halting the biosynthesis of pABA, i.e., p-aminobenzoic acid (a cofactor in folic acid biosynthesis) by irreversibly inhibiting the ADCS (4-amino-4-deoxychorismate synthase) enzyme of Chorismate pathway.[26] Based on origin, Abyssomicins are classified as either isolated from *Verrucosispora* (Abyssomicins B-L), or derived from *Streptomyces* (Abyssomicin E, and I, ent-homoabyssomicins A and B, Abyssomicins 2-5, M-X, and Neoabyssomicin A-C).[19,27-31] Till date, 32 Abyssomicins have been isolated from natural sources, and numerous have been synthesized. Although only limited biological activities of Abyssomicins have been reported, this pool of natural compounds serves as a good source to explore other biological activities.

In the present study, an attempt has been made to screen a library of Abyssomicins as a novel inhibitor of NDM-1 using computational approaches such as molecular modeling, molecular docking, ADMET profiling, molecular dynamics simulation, and free-energy calculations. We have identified Abyssomicin W and Neoabyssomicin B as the most potential inhibitors of NDM-1.

MATERIALS AND METHODS

Homology modeling, and preparation of protein and ligands

The FASTA sequence of NDM-1 prevalent in Saudi Arabia was retrieved from GenBank (ID: CP071280.1) (accessed on August 22, 2021) and submitted in SWISS-MODEL (accessed on August 22, 2021) to generate the model of NDM-1. The three-dimensional coordinates of 4EY2 were used as templates during homology modeling. The global and per-residue quality of the NDM-1 model was evaluated using the QMEAN scoring function (accessed on August 23, 2021).[32] The structure of the NDM-1 model was further verified using PSVS (Protein Structure Validation Suite), which comprises PROCHECK, MolProbity, VERIFY3D, Prosa II, and Ramachandran plot, (accessed on August 23, 2021).[33-38]

The structure of NDM-1 was preprocessed before molecular docking by removing any heteroatoms or non-catalytic water molecules, adding hydrogen atoms, and assigning Kollman charges. All these modifications were performed in AutoDock tools (ADT). Further, the overall energy of NDM-1 was minimized using CHARMM36 forcefield using the Discovery Studio visualizer. The 2D structure of all the ligands considered in this study was drawn in ChemDraw Ultra 7.0 (Perkin-Elmer, MA, USA). The structure of ligands was cleaned, and its energy was minimized using Universal Force Field (UFF) and converted to ready-to-dock format pdbqt using the ligand preparation function of PyRx 0.8 (SourceForge, CA, USA). The Gasteiger partial charges were added, non-polar H-atoms were merged, and rotatable bonds were defined using ADT.

Virtual screening and molecular docking

The interaction between NDM-1 and ligands was elucidated by molecular docking using AutoDock Vina assembled in PyRx 0.8 (SourceForge, CA, USA).[39-41] The grid box was defined by selecting the key amino acid residues of NDM-1 such as His120, His122, Asp124, His189, Cys208, and His250. The dimension of the grid box was set to 25.0 × 25.0 × 25.0 Å centered at 0.8 × 7.8 × 23.3 Å with 0.375 Å spacing. Molecular docking was performed using LGA (Lamarck Genetic Algorithm) for global search and Solis-Wets local search methods. For each run, 2500000 energy calculations were computed and a total of 10 docking runs were performed. The population size, translational step, quaternions, and torsions were set as 150, 0.2, 5, and 5, respectively. The van der Waals' and electrostatic parameters were calculated with the help of a distance-dependent dielectric function. The binding pattern and mode of interaction of top-scoring ligands were analyzed in BIOVIA Discovery Studio Visualizer v16.1.0.15350.

The dissociation constant (K_d) of ligands for proteins was estimated from docking energy (ΔG) using the following relation as reported earlier.[42,43]

$$\Delta G = -RT \ln K_d$$

Where R and T were universal gas constant (=1.987 cal/mol/K) and temperature (=298 K), respectively.

Validation of docking protocol

The validity of the docking protocol was confirmed by redocking the ligand (i.e., Methicillin) present in the crystal structure of 4EY2 and comparing the docked pose with the crystal structure pose by calculating RMSD. Methicillin occupied a similar pose at the active site of NDM-1

as present in the crystal structure. The RMSD between crystal structure pose and docking pose is estimated to be 0.8376 Å.

Determination of physico-chemical and ADMET properties

The physico-chemical and ADMET properties of the shortlisted ligands were determined using the SWISS-ADME server (http://www.swissadme.ch/index.php), (accessed on September 5, 2021). In physico-chemical properties, the parameters such as molecular weight (mol wt), the number of rotatable bonds (RB), hydrogen bond donors (HB donor), hydrogen bond acceptor (HB acceptor), total polar surface area (Tpsa), and lipophilicity (XlogP3) were determined. Likewise, in ADMET properties, parameters such as gastrointestinal (GI) absorption, blood-brain barrier (BBB) permeability, P-glycoprotein (P-gp) substrate, Cytochrome P450 1A2 inhibitor, Cytochrome P450 2C19 inhibitor, Cytochrome P450 2C9 inhibitor, Cytochrome P450 2D6 inhibitor, Cytochrome P450 3A4 inhibitor, and skin permeation (Log K_p) were determined. Moreover, it was also established whether the shortlisted ligands violated any of Lipinski's, Ghose's, Veber's, Egan's, and Muegge's rules. The Abbott bioavailability score, Pan assay interference structure (PAINS) alert, Brenk structural alert, lead likeness, and synthetic accessibility scores were also determined. The toxicological properties such as mutagenicity, tumorigenicity, reproductive effect, and irritability were determined with the help of the Datawarrior 5.5.0 tool (Allschwil, Switzerland).

Molecular dynamics (MD) simulation

GROMACS simulation package (GROMACS 2020.4) was used to perform molecular dynamics (MD) simulations. MD simulation of protein-ligand complexes (NDM-1 and Abyssomicin W, and NDM-1 and Neoabyssomicin B) was carried out for 100 ns using CHARMM36 forcefield; trajectory and energy files were written every 10 ps. The system was solvated in an octahedral box, containing TIP3P water molecules. The protein was centered in the simulation box within a minimum distance to the box edge of 1 nm to efficiently satisfy the minimum image convention. A simulation was performed in 0.15 M KCl by adding 30 Potassium ions and 24 Chloride ions in both systems. Overall NDM-1-Abyssomicin W system contained 29137 atoms and the NDM-1-Neoabyssomicin B system contained 29144 atoms. The protonation states were evaluated at 7.4 pH the using playmolecule web server (https://www.playmolecule.com/) for His, Lys, Arg, Asp and Glu residues and implemented after visual inspection. Minimization was carried out for 5000 steps using Steepest Descent Method and the convergence was achieved within the maximum force <1000 (KJ/mol/nm), to remove any steric clashes. The system was equilibrated at NVT and NPT ensembles for 100ps (50,000 steps) and 1000ps (1,000,000 steps), respectively, using time steps 0.2 and 0.1 fs, at 300K to ensure a fully converged system for a production run.

The production runs for simulation were carried out at a constant temperature of 300 K and a pressure of 1 atm or bar (NPT) using weak coupling velocity-rescaling (modified Berendsen thermostat) and Parrinello-Rahman algorithms, respectively. Relaxation times were set to τ T = 0.1 ps and τ *P* = 2.0 ps. All bond lengths involving hydrogen atoms were kept rigid at ideal bond lengths using the Linear Constraint Solver (LINCS) algorithm, allowing for a time step of 2 fs. Verlet scheme was used for the calculation of non-bonded interactions. Periodic Boundary Conditions (PBC) were used in all x, y, and z directions. Interactions within a short-range cutoff of 1.2 nm were calculated in each time step. Particle Mesh Ewald (PME) was used to calculate the electrostatic interactions and forces to account for a homogeneous medium outside the long-range cutoff. The production was run for 100 ns for both complexes.

Free energy calculation by MM-PBSA

Molecular Mechanics-Poisson Boltzmann surface area (MM-PBSA) of NDM-1 and Abyssomicin complexes was performed on a short stable MD trajectory, using g_mmpbsa package.[44] The following equation was used to calculate the free energy (ΔG_{Bind}) of NDM-1 and Abyssomicin complex formation:

$$\Delta G_{Bind} = G_{Complex} - (G_{protein} + G_{Ligand})$$

where, $G_{Complex}$, $G_{Protein}$ and G_{Ligand} are the free energies of the complex, protein, and ligand, respectively.

RESULTS AND DISCUSSION

Assessment of NDM-1 model generated by homology modelling

The three-dimensional model of NDM-1 was generated by homology modelling in SWISS-MODEL server in automated mode. In order to retrieve a suitable template, the amino acid sequence of NDM-1 isolate from Saudi Arabia (GenBank ID: CP071280.1) was used as a query sequence in SWISS-MODEL template library search with BLAST,[45] and HHblits.[46] Overall 643 templates were identified, amongst which the A-chain of 4EY2 was used as the template. The resolution, sequence identity, sequence similarity, and coverage score of 4EY2 template were 1.17 Å, 100, 0.61, and 1.00, respectively. Finally, the model was built based on target-template alignment as shown in Figure 1a using ProMod3, and validated by QMEAN4 score.[47] The normalized QMEAN4 score of NDM-1 model was compared with that of X-ray crystal structures of known proteins of different sizes [Figure 1b]. The QMEAN4 score of NDM-1 model was less than 1.00 (0.93), thereby indicating that the overall three-dimensional structure of NDM-1 model was compared with that of a protein resolved by X-ray crystallography. The generated model of NDM-1 was then subjected to a short time molecular dynamics simulation to relax any strains in the structure and to mimic the native conformation of the protein. Further, the NDM-1 model was evaluated by PSVS (Protein Structure Validation Suite) (https://montelionelab.chem.rpi.edu/PSVS/), which comprises various protein structure evaluation tools such as PROCHECK, Ramachandran plot, MolProbity, Verify3D, Prosa II, etc. The overall global quality of the NDM-1 model was reported as Z scores, which are based on high-resolution X-ray crystal structures. The Ramachandran

Table 1: Evaluation of NDM-1 model using PSVS (Protein Structure Validation Suite)

Parameters	Mean score	Z-score
Verify 3D	0.27	−3.05
ProsaII (−ve)	0.69	0.17
Procheck (ϕ–ψ)	−0.12	−0.16
Procheck (all)	−0.01	−0.06
Molprobity Clash score	0.85	1.38
RMSD_bond length (Å)	0.015	-
RMSD_bond angle (°)	2.0	-
Close contacts (within 2.2 Å)	0	-
Ramachandran plot summary (Procheck)		-
Most favored regions (%)	92.6	
Additionally allowed regions (%)	6.9	
Generously allowed regions (%)	0.0	
Disallowed regions	0.5	
Ramachandran plot statistics (Richardson's lab)		-
Most favored regions (%)	98.3	
Allowed regions (%)	1.3	
Disallowed regions (%)	0.4	

plot [Figure 1c] generated by Procheck showed that 92.6%, 6.9%, 0%, and 0.5% residues of NDM-1 model occupied the favoured regions, additionally allowed regions, generously allowed regions, and disallowed regions, respectively. Similarly, the Ramachandran plot statistics by Richardson's lab confirmed that 98.3% of residues were placed in the most favoured regions, while 1.3% and 0.4% of residues occupied allowed and disallowed regions respectively [Table 1]. The superimposition of NDM-1 model and 4EY2 template revealed that the two structures had identical conformation, with all the key amino acid residues in a proper position and orientation [Figure 1d]. The results confirmed that the overall quality of NDM-1 model was good and therefore can be used in molecular docking studies.

Analysis of virtual screening

The basis of structure-based drug design is the virtual screening of a set of potential ligands against the protein of interest.[48] In this study, the potential of Abyssomicins as novel inhibitors of NDM-1 was evaluated by virtual screening using AutoDock Vina. The binding energy of all the ligands is listed in Table 2. The binding energies of different ligands vary from −6.7 to −9.6 kcal/mol, suggesting moderate to the high affinity of Abyssomicins towards NDM-1. An analysis of docking energy revealed that the top 3 (or top 10%) ligands showing the highest binding affinity for NDM-1 were Abyssomicin J, Abyssomicin W, and Neoabyssomicin B, having binding energies of −9.4, −9.6, and −9.5 kcal/mol, respectively. These ligands were selected for further screening by physico-chemical and ADMET properties.

Table 2: Virtual screening of Abyssomicins against NDM-1

Ligand	Binding energy (kcal/mol)
Methicilin_hydrolyzed (Control)	−7.3
Abyssomicin 2	−8.0
Abyssomicin 3	−7.7
Abyssomicin 4	−7.7
Abyssomicin 5	−7.8
Abyssomicin B	−8.3
Abyssomicin C	−7.7
Abyssomicin D	−8.4
Abyssomicin E	−7.8
Abyssomicin G	−8.2
Abyssomicin H	−7.7
Abyssomicin I	−7.5
Abyssomicin J	**−9.4**
Abyssomicin K	−7.7
Abyssomicin L	−7.9
Abyssomicin T	−7.6
Abyssomicin U	−7.3
Abyssomicin V	−7.3
Abyssomicin W	**−9.6**
Abyssomicin X	−7.5
Abyssomicin Y	−8.4
Atrop-abyssomicin C	−7.8
Iso-abyssomicin D	−8.2
Neoabyssomicin B	**−9.5**
Neoabyssomicin C	−6.7
Neoabyssomicin D	−7.0
Neoabyssomicin M	−8.1
Neoabyssomicin N	−8.1
Neoabyssomicin O	−7.6
Neoabyssomicin P	−7.6
Neoabyssomicin Q	−7.1
Neoabyssomicin R	−7.0
Neoabyssomicin S	−7.4
Oxidized abyssomicin I	−7.3

Ligands in bold were selected for further analysis

Analysis of physico-chemical and ADMET properties

The utilization of computational tools to study the physico-chemical and ADEMT properties of a molecule is widely reported.[49] In the present study, the physico-chemical and ADMET properties of the ligands with the lowest binding energy in the virtual screening i.e. Abyssomicin J, Abyssomicin W and Neoabyssomicin B, were evaluated using SwissADMET. An analysis of the physico-chemical properties of the shortlisted ligands suggested that Abyssomicin J violated three Lipinski's rule of five; it had a molecular weight of 712.80 g/mol, 12 hydrogen bond acceptors, and a total polar surface area of 211.42 Å^2 [Table 3]. The physico-chemical properties of Abyssomicin W such as molecular weight, rotatable bonds, hydrogen bond donors, hydrogen bond acceptors, Tpsa and XlogP3 were 392.44 g/mol, 0, 3, 7, 121.13 Å^2, and 1.06, respectively. Similarly, the physico-chemical properties of Neoabyssomicin B such as molecular weight, rotatable bonds, hydrogen bond donors, hydrogen bond acceptors, Tpsa and XlogP3 were 362.37 g/mol, 0, 1, 7, 99.13 Å^2, and 1.05, respectively. Abyssomicin J was moderately soluble, while Abyssomicin W and Neoabyssomicin B were soluble. Also, the pharmacokinetic properties such as GI absorption and skin permeability of Abyssomicin J were much different than the other two ligands namely Abyssomicin W and Neoabyssomicin B [Table 4]. Other pharmacokinetic properties such as blood-brain barrier, P-glycoprotein substrate potential, an inhibitor of CYC1A2, CYP2C19, CYP2C9, CYP2D6, and CYP3A4 of all the three ligands were similar. Further, the analysis of drug-likeness and medicinal properties suggested that Abyssomicin J was not a suitable candidate drug molecule, as it violates Lipinski's, Ghose's, Veber's, Egan's, and Muegge's rules [Table 5]. Moreover, the bioavailability score and synthetic accessibility of Abyssomicin J were much lower than Abyssomicin W and Neoabyssomicin B. Since, the physico-chemical, pharmacokinetic, druglikeness, and medicinal properties of Abyssomicin W and Neoabyssomicin B were within acceptable limits, we finalized these two molecules for further experiments by molecular docking, molecular dynamics simulation, and free energy calculation.

Analysis of molecular docking

An analysis of the three-dimensional structure of NDM-1 suggested that it has a four-layered αβ/βα MBL fold.[50] NDM-1 has a deep and wide active site with two bound Zn ions, namely Zn1 and Zn2. The Zn1 ion is coordinated with His120, His122, His189, and Asp124 in a tetrahedral geometry, while Zn2 ion is coordinated with Cys208, His250, and Asp124 in a trigonal pyramidal geometry. A water molecule or a hydroxide moiety located between Zn1 and Zn2 acts as a nucleophile during the hydrolysis of β-lactam ring of antibiotics[50] In addition to the active site residues, several other residues around it such as Leu65, Met67, Pro68, Val73, Gly69, Phe70, Trp93, Leu209, Ile210, Lys211, Asp212, Lys214, Ala215, Lys216, and Asn220 have been proposed to play a crucial role in the hydrolysis of β-lactam ring.[2] In this study, we performed molecular docking of Abyssomicin W and Neoabyssomicin B along with the control ligand (hydrolyzed Methicillin) by placing the grid box at the active site of NDM-1, and the results are presented in Figures 2 and 3 and Table 6. All the ligands were found to bind the active site of NDM-1 [Figure 2a, b].

Methicillin (control) and NDM-1 interaction

The crystal structure of NDM-1 (PDB ID: 4EY2) reported a hydrolyzed Methicillin at the active site.[51] We extracted the hydrolyzed Methicillin from the crystal structure and re-docked again along with other Abyssomicin ligands. The analysis of re-docked

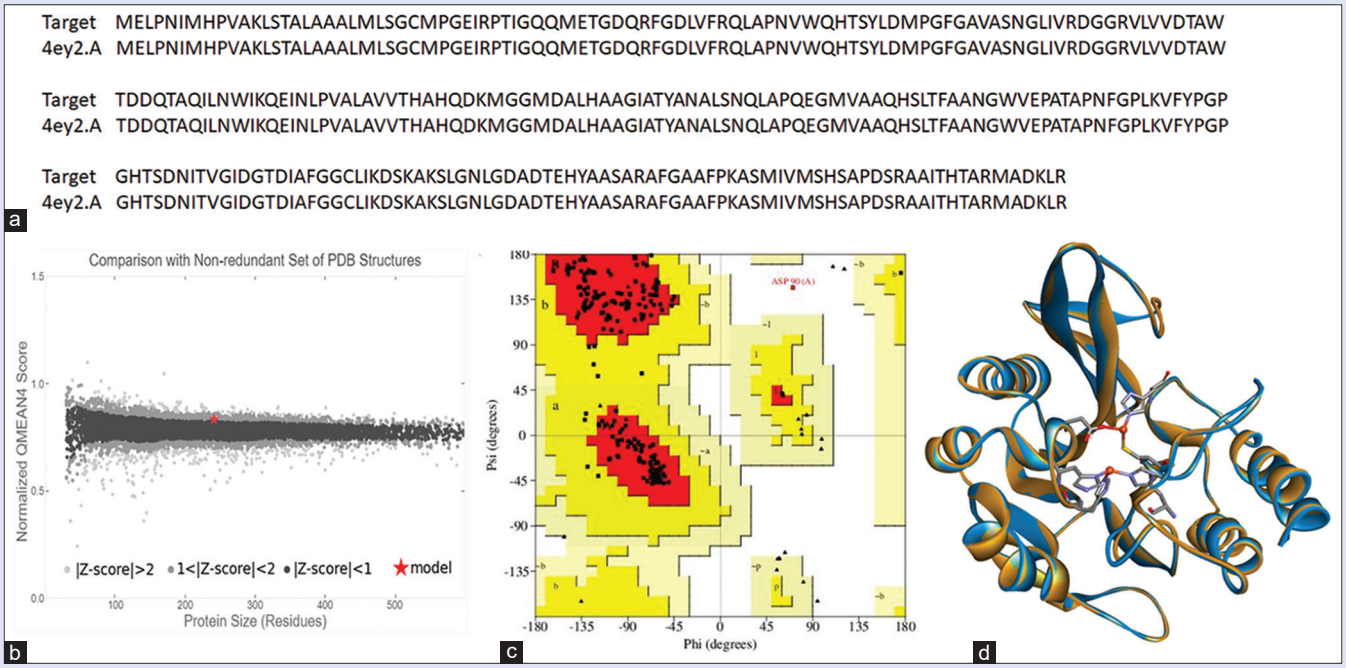

Figure 1: Molecular modeling of NDM-1 isolate reported from Saudi Arabia. (a) Sequence alignment between the template (PDB ID: 4EY2) and target using Clustal Omega, (b) Validation of the model by QMEAN4, (c) Ramachandran plot of the modeled NDM-1, generated using ProCheck, and (d) Superimposition of the modeled NDM-1 over the template (PDB ID: 4EY2) structure. The active site residues are represented as sticks

Table 3: Physico-chemical properties of the shortlisted Abyssomicins

Name and structure of molecule	Mol wt (g/mol)	RB	HB donor	HB acceptor	Tpsa (Å^2)	XlogP3	Solubility (log S)
Abyssomicin J	712.80	2	4	12	211.42	3.98	Moderately soluble
Abyssomicin W	392.44	0	3	7	121.13	1.06	Soluble
Neoabyssomicin B	362.37	0	1	7	99.13	1.05	Soluble

Table 4: Pharmacokinetic properties of the shortlisted Abyssomicins

Properties	Abyssomicin J	Abyssomicin W	Neoabyssomicin B
GI absorption	Low	High	High
BBB permeability	No	No	No
P-gp substrate	Yes	Yes	Yes
CYP1A2 inhibitor	No	No	No
CYP2C19 inhibitor	No	No	No
CYP2C9 inhibitor	No	No	No
CYP2D6 inhibitor	No	No	No
CYP3A4 inhibitor	No	No	No
Skin permeability (log *Kp*)	−9.35 cm/s	−7.94 cm/s	−7.76 cm/s

Table 5: Drug-likeness and medicinal properties of the shortlisted Abyssomicins

Properties	Abyssomicin J	Abyssomicin W	Neoabyssomicin B
Lipinski's rule	2	0	0
Ghose's rule	3	0	0
Veber's rule	1	0	0
Egan's rule	1	0	0
Muegge's rule	4	0	0
Bioavailability score	0.11	0.56	0.56
PAINS alert	0	0	0
Brenk alert	1	0	2
Leadlikeness alert	1	0	0
Synthetic accessibility	9.56	6.31	6.62

hydrolyzed Methicillin to NDM-1 revealed that it occupied a similar position at the active site as reported in the crystal structure. The RMSD between the re-docked pose and crystal structure pose of hydrolyzed Methicillin was 0.8376 Å. The Methicillin-NDM-1 complex was stabilized primarily by hydrogen bonding. Methicillin formed seven conventional hydrogen bonds (strong H-bonds) with His122:HD1 (2.23 Å), Gln123:HN (2.45 Å and 2.10 Å), Asp124:HN (2.06 Å), Asp124:OD2 (2.91 Å), His189:HE2 (2.41 Å), and Asn220:HN (2.02 Å) along with two carbon-hydrogen bonds (weak H-bonds) with Glu152:O (3.61 Å), and Glu152:OE1 (3.47 Å) [Table 6]. In addition, there was a metal-acceptor interaction between Zn1 and O-atom of hydrolyzed Methicillin (2.23 Å). The protein-ligand complex was further stabilized by two hydrophobic interactions with Trp93 (5.62 Å) and Val73 (4.50 Å). Moreover, van der Waals' interactions were formed by Ile35, Leu65, Met67, His120, Met154, Cys208, Leu218, Gly219, and His250 [Figure 2c]. The binding energy and the binding affinity of hydrolyzed Methicillin towards NDM-1 were estimated to be −7.3 kcal/mol, and 2.26×10^5 M^{-1}, respectively.

Abyssomicin W and NDM-1 interaction

The Abyssomicin W-NDM-1 complex was stabilized mainly by hydrophobic interactions. Abyssomicin W formed four hydrophobic interactions with His122 (3.84 Å), Ile35 (4.01 Å and 4.18 Å), and Phe70 (5.25 Å) [Table 6]. In addition, there were two metal-acceptor interactions between Zn2 and O-atom of Abyssomicin W (1.69 Å and 3.16 Å). The protein-ligand complex was further stabilized by one conventional hydrogen bond (strong H-bond) with His250:HE2 (2.28 Å). Moreover, van der Waals' interactions were formed by Leu65, Met67, Val73, Trp93, His120, Gln123, Asp124, His189, Cys208, Lys211, Gly219, and Asn220 [Figure 3a]. The binding energy and the binding affinity of Abyssomicin W towards NDM-1 were estimated to be −9.6 kcal/mol and 1.10×10^6 M^{-1}, respectively.

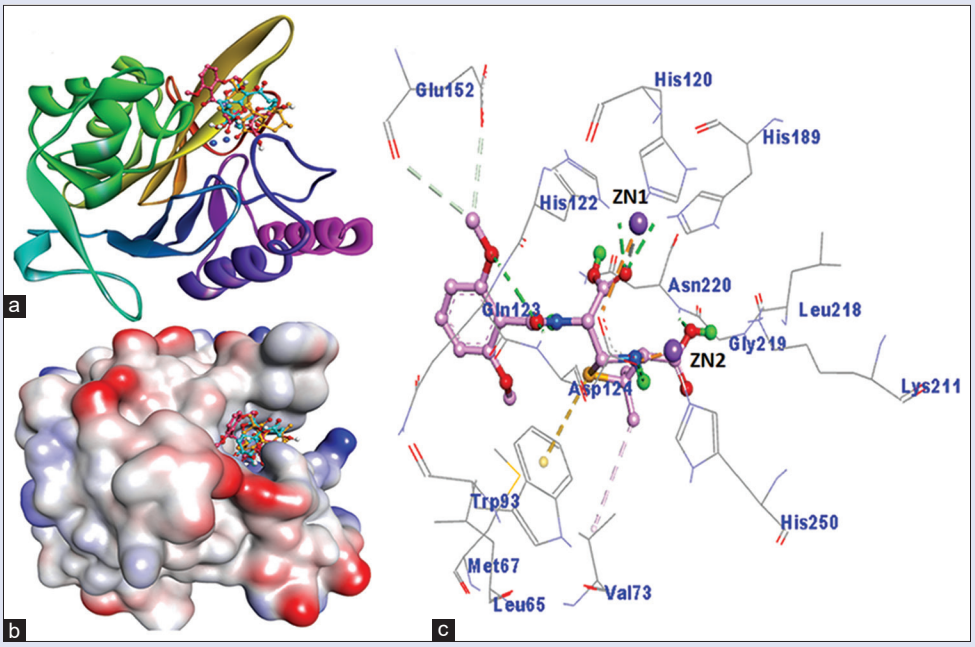

Figure 2: Molecular docking of hydrolyzed Methicillin (control), Abyssomicin W and Neoabyssomicin B at the active site of NDM-1. (a) 2D representation of the binding of ligands, (b) 3D representation of the active site of NDM-1 with bound ligands, and (c) Interaction between NDM-1 and hydrolyzed Methicillin

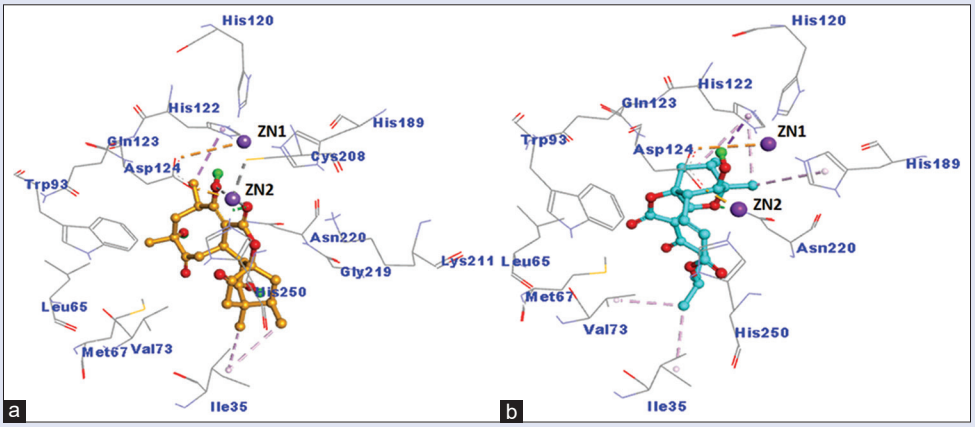

Figure 3: Molecular interaction of NDM-1 with (a) Abyssomicin W, and (b) Neoabyssomicin B

Table 6: Molecular docking parameters for the interaction between NDM-1 and Abyssomicins

Interaction between Donor-Acceptor atoms	Distance (Å)	Nature of Interaction	Docking energy, kcal/mol	Dissociation constant, M^{-1}
NDM-1 and Methicillin interaction				
HIS122:HD1 - LIG: O	2.23	Hydrogen Bond	−7.3	2.26×10^5
GLN123:HN - LIG: O	2.45	Hydrogen Bond		
GLN123:HN - LIG: O	2.10	Hydrogen Bond		
ASP124:HN - LIG: O	2.06	Hydrogen Bond		
HIS189:HE2 - LIG: O	2.41	Hydrogen Bond		
ASN220:HN - LIG: O	2.02	Hydrogen Bond		
LIG: H - ASP124:OD2	2.91	Hydrogen Bond		
LIG: C - GLU152:O	3.61	Carbon Hydrogen Bond		
LIG: C - GLU152:OE1	3.47	Carbon Hydrogen Bond		
ZN1:ZN - LIG: O	2.23	Metal-Acceptor		
LIG: S - TRP93	5.62	Hydrophobic (Pi-Sulfur)		
LIG: C - VAL73	4.50	Hydrophobic (Alkyl)		
NDM-1 and Abyssomicin W interaction				
HIS250:HE2 - LIG: O	2.28	Hydrogen Bond	−9.6	1.10×10^7
ZN2:ZN - LIG: O	1.69	Metal-Acceptor		
ZN2:ZN - LIG: O	3.16	Metal-Acceptor		
LIG: C - HIS122	3.84	Hydrophobic (Pi-Sigma)		
LIG: C - ILE35	4.01	Hydrophobic (Alkyl)		
LIG: C - ILE35	4.18	Hydrophobic (Alkyl)		
PHE70 - LIG: C	5.25	Hydrophobic (Pi-Alkyl)		
NDM-1 and Neoabyssomicin B interaction				
ASN220:HD22 - LIG: O	1.97	Hydrogen Bond	−9.5	9.28×10^6
LIG: C - HIS122	3.72	Hydrophobic (Pi-Sigma)		
LIG: C - ILE35	3.92	Hydrophobic (Alkyl)		
LIG: C - VAL73	4.02	Hydrophobic (Alkyl)		
HIS122 - LIG	4.04	Hydrophobic (Pi-Alkyl)		
HIS122 - LIG: C	4.08	Hydrophobic (Pi-Alkyl)		
HIS189 - LIG: C	4.43	Hydrophobic (Pi-Alkyl)		

Neoabyssomicin B and NDM-1 interaction

The Neoabyssomicin B-NDM-1 complex was stabilized principally by hydrophobic interactions. Neoabyssomicin B formed six hydrophobic interactions with His122 (3.72 Å, 4.04 Å, and 4.08 Å), Ile35 (3.92 Å), Val73 (4.02 Å), and His189 (4.43 Å) [Table 6]. In addition, Neoabyssomicin B formed one conventional hydrogen bond (strong H-bond) with Asn220:HD22 (1.97 Å). The protein-ligand complex was further stabilized by van der Waals' interactions formed by Leu65, Met67, Trp93, His120, Gln123, Asp124, and His250 [Figure 3b]. The binding energy and the binding affinity of Neoabyssomicin B towards NDM-1 were estimated to be −8.5 kcal/mol and 9.28×10^6 M^{-1}, respectively.

Analysis of molecular dynamics (MD) simulation

The structure and dynamics of protein-ligand complexes were analyzed by performing MD simulation for 100 ns and the results are discussed below.

Root mean square deviation (RMSD) analysis

The interaction of a ligand to a protein may lead to large conformational changes in the protein. This is often measured by calculating the deviation in protein's structure with respect to the initial docking frame (defined as RMSD) as a function of simulation time. In the present study, RMSD in Cα-atoms of NDM-1 alone, NDM-1-Abyssomicin W complex, NDM-1-Neoabyssomicin B complex, Abyssomicin W, and Neoabyssomicin B were measured during MD simulation [Figure 4a]. There were no significant fluctuations in the RMSD values of protein-ligand complex and ligands during the 100 ns MD simulation. The mean RMSD values (between 20-100 ns) of NDM-1 alone, NDM-1-Abyssomicin W complex, NDM-1-Neoabyssomicin B complex, Abyssomicin W alone, and Neoabyssomicin B were computed as 1.34 ± 0.28 Å, 1.53 ± 0.33 Å, 1.48 ± 0.36 Å, 0.68 ± 0.11 Å, and 0.72 ± 0.07 Å, respectively [Figure 4a]. Since the fluctuation in RMSD values of NDM-1-Abyssomicin complexes was within the acceptable limit, stable protein-ligand complexes are anticipated.

Root mean square fluctuation (RMSF) analysis

RMSF is a measurement of fluctuations in the protein's side chains due to the binding of a ligand. Figure 4b shows RMSF of NDM-1 in the presence of Abyssomicin W and Neoabyssomicin B during MD simulation. The higher RMSF values at the N- and C-terminal ends were due to greater flexibility at the terminals. Some minor fluctuations in RMSF of NDM-1 were observed, which might be due to the entry/binding of Abyssomicin W and Neoabyssomicin B to the active site located in the deep groove of the protein. The peaks observed in RMSF plot were located in the loop regions of NDM-1, which clearly have higher mobility.

Radius of gyration (Rg) and solvent accessible surface area (SASA) analysis

Radius of gyration (Rg) is a measure of protein's overall conformation and folding state due to the binding of a ligand. In this study, Rg of

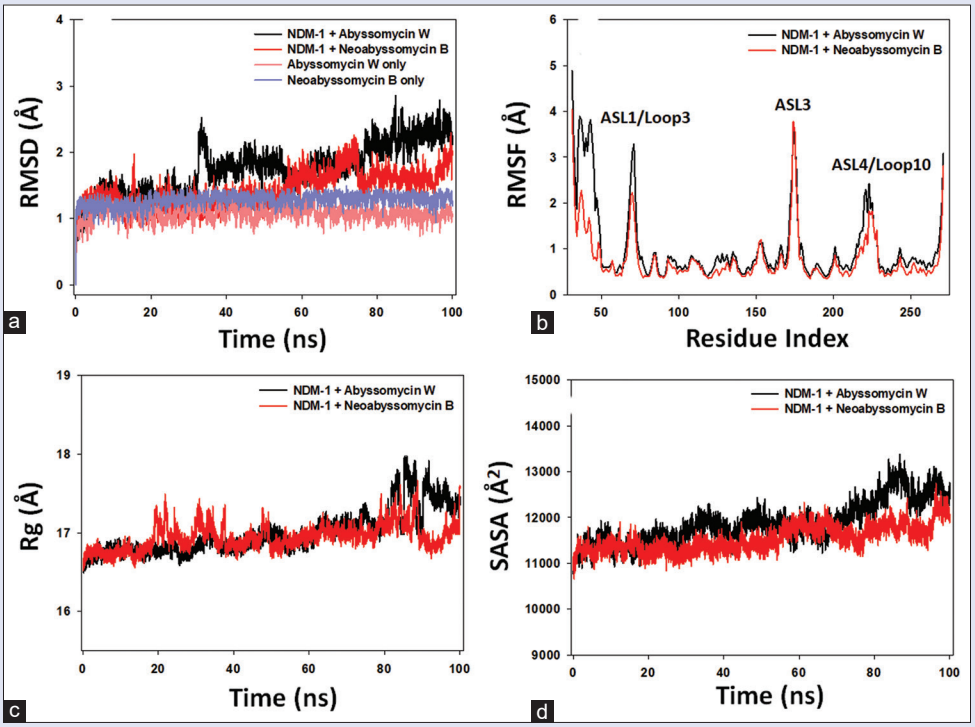

Figure 4: Molecular dynamics (MD) simulation of NDM-1 in complex with Abyssomicin W and Neoabyssomicin B. (a) Root mean square deviation (RMSD), (b) Root mean square fluctuation (RMSF), (c) Radius of gyration (Rg), and (d) Solvent accessible surface area (SASA)

protein-ligand complexes were measured to evaluate the compactness of protein during MD simulation [Figure 4c]. The average Rg values of NDM-1 alone, NDM-1-Abyssomicin W and NDM-1-Neoabyssomicin B complexes were estimated to be 16.23 ± 0.28 Å, 15.80 ± 0.36 Å and 15.73 ± 0.22, respectively. Also, SASA is another parameter to measure the overall packing and conformation of a protein under different conditions. Here, SASA of NDM-1 alone and with its Abyssomicin W and Neoabyssomicin B complexes were measured during MD simulation to explore the exposure of the protein to the solvent molecules and thus to access its conformational stability [Figure 4d]. Although, the values of SASA fluctuated during MD simulation, they remained within acceptable limits. The average SASA values of NDM-1 alone, NDM-1-Abyssomicin W and NDM-1-Neoabyssomicin B complexes were 11858 ± 463 Å^2, 11321 ± 371 Å^2, and 11687 ± 273 Å^2, respectively. The results of Rg and SASA confirmed the formation of stable NDM-1-Abyssomicin W and NDM-1-Neoabyssomicin B complexes.

Analysis of free energy (MM-PBSA) calculations

The binding free energy of a protein-ligand complex is governed by the thermodynamic contribution of the ligand inside the binding pocket of the protein. In this study, the binding thermodynamics of Abyssomicin W and Neoabyssomicin B alone towards NDM-1 was estimated using MM-PBSA approach. The binding free energy (ΔG_{Bind}) is defined as the difference in the free energy of the protein-ligand complexes and the sum of the free energies of protein and ligand.

$$\Delta G_{Bind} = G_{Complex} - (G_{Protein} + G_{Ligand})$$

ΔG_{Bind} can also be defined as the difference in enthalpic (ΔH) and entropic ($T\Delta S$) contributions.

$$\Delta G_{Bind} = \Delta H - T\,\Delta\, S$$

Further, the enthalpic contribution to free energy comprises energy of the gas phase (ΔEgas), and solvation free energy (ΔG_{sol}).

$$\Delta H = \Delta E_{gas} + \Delta G_{sol}$$

The gas phase energy is the sum of the internal energy (E_{int}), van der Waals' energy (E_{vdW}), and coulomb or electrostatic energy (E_{elec}).

$$\Delta E_{gas} = E_{int} + E_{vdW} + E_{elec}$$

Moreover, solvation free energy (ΔG_{sol}) is the sum of the polar (G_{polar}), and non-polar solvation energies ($G_{non\text{-}polar}$). The non-polar solvation free energy ($G_{non\text{-}polar}$) is defined as the sum of the surface tension proportionally constant (γ) multiplied by the value of SASA and the non-linear solvation free energy of a point solute (β).

$$\Delta G_{sol} = G_{polar} + G_{non\text{-}polar}$$

$$G_{non\text{-}polar} = \gamma SASA + \beta$$

In this study, the polar solvation free energy (G_{polar}) was estimated by Poisson-Boltzmann (PB) solvation model, while the values of γ and β were taken as 0.00542 kcal/mol and 0, respectively. Also, SASA was determined with the help of a linear combination of pairwise overlap (LCPO) model. The binding free energies (ΔG_{bind}) of Abyssomicin W and Neoabyssomicin B towards NDM-1 were −20.93 and −20.96 kcal/mol, indicating a strong interaction between protein and ligands [Table 7]. The decomposition of binding free energy (ΔG_{bind}) into its constituents revealed that the gas phase energy of Abyssomicin W (ΔE_{gas} = −17.84 kcal/mol) and Neoabyssomicin B (ΔE_{gas} = −17.83 kcal/mol) favored the formation of protein-ligand complexes.

In summary, Abyssomicins have been known to possess antimicrobial activities against Gram-positive bacteria and mycobacteria. A recent renewed interest in Abyssomicins have led to the identification of other biological activities such as antitumor and antiviral activities. Among the Abyssomicins, 4 natural Abyssomicins i.e. 2, C, J, and atrop-Abyssomicin C and nine synthetic derivatives of them have been reported to be biologically active against *Micrococcus luteus, Bacillus thuringiensis, Enterococcus faecalis*, MRSA,

Table 7: Free energy calculations (MM-PBSA) of NDM-1 in complex with Abyssomicin W and Neoabyssomicin B

Ligands	Binding free energy (*ΔGbind*)	Solvation energy (*ΔGsol*)	Gas-phase energy (*ΔEgas*)	Coulomb energy (*ΔEelec*)	van der Waals energy (*ΔEvdW*)	Polar solvation energy (*ΔGpolar*)	Non-polar solvation energy (*ΔGnon-polar*)
Abyssomicin W	−20.93	−3.09	−17.84	−16.19	−1.65	−3.17	0.08
Neoabyssomicin B	−20.96	−3.13	−17.83	−16.14	−1.69	−3.21	0.08

All the energies are in kcal/mol

VRSA (Vancomycin-resistant *S. aureus*), *Mycobacterium smegmatis, M. bovis* BCG (Bacille Calmette Guerin), and *M. tuberculosis*. Abyssomicins 2–5 have been shown to possess noncanonical reactivator activity of latent HIV. Similarly, the antitumor cell invasion abilities have been recorded for Abyssomicin I and its oxidized derivatives. Abyssomicins possess antimicrobial and antimycobacterial activities by the virtue of their ability to inhibit the synthesis of pABA (p-aminobenzoic acid) in the Chorismate pathway. Generally, they bind to ADCS via Michael addition to Cys263 residue. Although, Abyssomicins are known for antimicrobial and antimycobacterial activities, there is a wide scope to look for novel properties. Keeping this in mind, we explored the potential of Abyssomicins to inhibit β-lactamase (NDM-1), which is the primary reason for antibiotic resistance in Gram-negative bacteria. NDM-1 is a versatile enzyme which can hydrolyze almost all β-lactam antibiotics. The hydrolysis of β-lactam antibiotics by NDM-1 is initiated after the recognition and binding of substrate in the cavity near to Zn1 site (coordinated with His120, His122, and His189). Then, the carbonyl group of the substrate coordinates with Zn1 and increases its coordination number from 4 to 5, which in turn activate the carbonyl group of the β-lactam ring for nucleophilic attack. The hydroxide ion which attacks the carbonyl group is generated by the deprotonation of the metal-bound water molecule by Asp124. Conversely, Zn2 (bound with Asp124, Cys208, and His250) coordinates with the carboxy group of the β-lactam ring and stabilizes the transition state. Finally, Asp124 provides a proton to the penultimate amino N-atom to release the hydrolyzed product. In sum, the molecular docking results confirmed that Abyssomicin W and Neoabyssomicin B interacted with some of the key catalytic and active site residues such as His120, His122, Asp124, His189, Cys208 and His250 of NDM-1. In addition, Zn2 of NDM-1 was found to interact with Abyssomicin W. Since, Abyssomicin W and Neoabyssomicin B interfere with the catalytic mechanism of hydrolysis, they could be developed as mechanism-based inhibitors of NDM-1.

CONCLUSION

Structure-based drug design is a promising approach to identify novel therapeutic intervention against different diseases in a timely and cost-effective manner. In this study, we have made an attempt to identify novel inhibitors against NDM-1, an enzyme commonly found in multi-drug resistance bacteria. For this purpose, we have generated a model of NDM-1 protein on the basis of blaNDM-1 gene prevalent in Saudi Arabia. Virtual screening of Abyssomicins has been performed to shortlist novel molecules with a good ability to bind the active site of NDM-1. The initial screening has led to the identification of three molecules namely Abyssomicin J, Abyssomicin W, and Neoabyssomicin S. Further screening of these molecules by physico-chemical properties, and ADMET properties like pharmacokinetics, druglikeness, and medicinal properties suggests that only Abyssomicin W and Neoabyssomicin B obey the Lipinski's rule of five. An analysis of molecular docking suggests that Abyssomicin W and Neoabyssomicin B interact with key catalytic residues of NDM-1 and occupy the same binding pocketas done by Methicillin (control ligand). Molecular dynamics simulation and free energy calculations suggest that Abyssomicin W and Neoabyssomicin B formed a stable conformation within the catalytic pocket of NDM-1. Overall, the findings of this study suggest the possible use of Abyssomicin W and Neoabyssomicin B as a scaffold for the development of more potent inhibitors of NDM-1 which may serve as a novel therapeutic intervention in addressing antibiotic resistance problem.

Acknowledgements

"The authors extend their acknowledgement to the Deanship of Scientific Research, Vice Presidency for Graduate Studies and Scientific Research, King Faisal University, Saudi Arabia (Project No. GRANT273)".

Financial support and sponsorship

This work was supported by the Deanship of Scientific Research, Vice Presidency for Graduate Studies and Scientific Research, King Faisal University, Saudi Arabia (Grant273).

Conflicts of interest

There are no conflicts of interest.

REFERENCES

1. Faheem M, Rehman MT, Danishuddin M, Khan AU. Biochemical characterization of CTX-M-15 from Enterobacter cloacae and designing a novel non-β-lactam-β-lactamase inhibitor. PLoS One 2013;8:e56926. doi: 10.1371/journal.pone. 0056926.
2. Khan AU, Rehman MT. Role of non-active-site residue Trp-93 in the function and stability of New Delhi metallo-β-lactamase 1. Antimicrob Agents Chemother 2016;60:356-60.
3. Rehman MT, Alajmi MF, Hussain A, Rather GM, Khan MA. High-throughput virtual screening, molecular dynamics simulation, and enzyme kinetics identified ZINC84525623 as a potential inhibitor of NDM-1. Int J Mol Sci 2019;20:819.
4. Gould IM, Bal AM. New antibiotic agents in the pipeline and how they can help overcome microbial resistance. Virulence 2013;4:185-91.
5. Viswanathan VK. Off-label abuse of antibiotics by bacteria. Gut Microbes 2014;5:3-4.
6. Michael CA, Dominey-Howes D, Labbate M. The antimicrobial resistance crisis: Causes, consequences, and management. Front Public Health 2014;2:145.
7. Rossolini GM, Arena F, Pecile P, Pollini S. Update on the antibiotic resistance crisis. Curr Opin Pharmacol 2014;18:56-60.
8. Gross M. Antibiotics in crisis. Curr Biol 2013;23:R1063-5. doi: 10.1016/j.cub. 2013.11.057.
9. Muteeb G, Rehman MT, Ali SZ, Al-Shahrani AM, Kamal MA, Ashraf GM. Phage display technique: A novel medicinal approach to overcome antibiotic resistance by using peptide-based inhibitors against β-lactamases. Curr Drug Metab 2017;18:90-5.
10. Ahmed MZ, Muteeb G, Khan S, Alqahtani AS, Somvanshi P, Alqahtani MS, *et al.* Identifying novel inhibitor of quorum sensing transcriptional regulator (SdiA) of Klebsiella pneumoniae through modelling, docking and molecular dynamics simulation. J Biomol Struct Dyn 2021;39:3594-604.
11. Ambler RP. The structure of β-lactamases. Philos Trans R Soc Lond B Biol Sci 1980;289:321-31.
12. Bush K, Jacoby GA. Updated functional classification of β-lactamases. Antimicrob Agents Chemother 2010;54:969-76.
13. Kumarasamy KK, Toleman MA, Walsh TR, Bagaria J, Butt F, Balakrishnan R, *et al.* Emergence of a new antibiotic resistance mechanism in India, Pakistan, and the UK: A molecular, biological, and epidemiological study. Lancet Infect Dis 2010;10:597-602.
14. Shibl A, Al-Agamy M, Memish Z, Senok A, Khader SA, Assiri A. The emergence of OXA-48- and NDM-1-positive Klebsiella pneumoniae in Riyadh, Saudi Arabia. Int J Infect Dis 2013;17:e1130-3. doi: 10.1016/j.ijid. 2013.06.016.

15. Poirel L, Al Maskari Z, Al Rashdi F, Bernabeu S, Nordmann P. NDM-1-producing Klebsiella pneumoniae isolated in the Sultanate of Oman. J Antimicrob Chemother 2011;66:304-6.
16. Jamal W, Rotimi VO, Albert MJ, Khodakhast F, Udo EE, Poirel L. Emergence of nosocomial New Delhi metallo-β-lactamase-1 (NDM-1)-producing Klebsiella pneumoniae in patients admitted to a tertiary care hospital in Kuwait. Int J Antimicrob Agents 2012;39:183-4.
17. El-Herte RI, Araj GF, Matar GM, Baroud M, Kanafani ZA, Kanj SS. Detection of carbapenem-resistant *Escherichia coli* and Klebsiella pneumoniae producing NDM-1 in Lebanon. J Infect Dev Ctries 2012;6:457-61.
18. Dortet L, Poirel L, Al Yaqoubi F, Nordmann P. NDM-1, OXA-48 and OXA-181 carbapenemase-producing Enterobacteriaceae in Sultanate of Oman. Clin Microbiol Infect 2012;18:E144-8. doi: 10.1111/j. 1469-0691.2012.03796.x.
19. León B, Navarro G, Dickey BJ, Stepan G, Tsai A, Jones GS, *et al.* Abyssomicin 2 reactivates latent HIV-1 by a PKC- and HDAC-independent mechanism. Org Lett 2015;17:262-5.
20. Lacoske MH, Theodorakis EA. Spirotetronate polyketides as leads in drug discovery. J Nat Prod 2015;78:562-75.
21. Vieweg L, Reichau S, Schobert R, Leadlay PF, Süssmuth RD. Recent advances in the field of bioactive tetronates. Nat Prod Rep 2014;31:1554-84.
22. Bister B, Bischoff D, Ströbele M, Riedlinger J, Reicke A, Wolter F, *et al.* Abyssomicin C—A polycyclic antibiotic from a marineverrucosispora strain as an inhibitor of thep-Aminobenzoic Acid/tetrahydrofolate biosynthesis pathway. Angew Chem Int Ed Engl 2004;43:2574-6.
23. Riedlinger J, Reicke A, Zähner H, Krismer B, Bull AT, Maldonado LA, *et al.* Abyssomicins, inhibitors of the para-aminobenzoic acid pathway produced by the marine Verrucosispora strain AB-18-032. J Antibiot (Tokyo) 2004;57:271-9.
24. Wang Q, Song F, Xiao X, Huang P, Li L, Monte A, *et al.* Abyssomicins from the South China Sea deep-sea sediment Verrucosispora sp.: Natural thioether Michael addition adducts as antitubercular prodrugs. Angew Chem Int Ed Engl 2013;52:1231-4.
25. Freundlich JS, Lalgondar M, Wei JR, Swanson S, Sorensen EJ, Rubin EJ, *et al.* The Abyssomicin C family as *in vitro* inhibitors of Mycobacterium tuberculosis. Tuberculosis (Edinb) 2010;90:298-300.
26. Bihelovic F, Karadzic I, Matovic R, Saicic RN. Total synthesis and biological evaluation of (–)-atrop–abyssomicin C. Org Biomol Chem 2013;11:5413-24.
27. Igarashi Y, Yu L, Miyanaga S, Fukuda T, Saitoh N, Sakurai H, *et al.* Abyssomicin I, a modified polycyclic polyketide from Streptomyces sp. CHI39. J Nat Prod 2010;73:1943-6.
28. Abdalla MA, Yadav PP, Dittrich B, Schüffler A, Laatsch H. ent -Homoabyssomicins A and B, Two new spirotetronate metabolites from streptomyces sp. Ank 210. Org Lett 2011;13:2156-9.
29. Wang X, Elshahawi SI, Cai W, Zhang Y, Ponomareva LV, Chen X, *et al.* Bi- and Tetracyclic spirotetronates from the coal mine fire isolate streptomyces sp. LC-6-2. J Nat Prod 2017;80:1141-9.
30. Song Y, Li Q, Qin F, Sun C, Liang H, Wei X, *et al.* Neoabyssomicins A–C, polycyclic macrolactones from the deep-sea derived Streptomyces koyangensis SCSIO 5802. Tetrahedron 2017;73:5366-72.
31. Niu XM, Li SH, Görls H, Schollmeyer D, Hilliger M, Grabley S, *et al.* Abyssomicin E, a highly functionalized polycyclic metabolite from Streptomyces species. Org Lett 2007;9:2437-40.
32. Studer G, Rempfer C, Waterhouse AM, Gumienny R, Haas J, Schwede T. QMEANDisCo-distance constraints applied on model quality estimation. Bioinformatics 2020;36:1765-71.
33. Bhattacharya A, Tejero R, Montelione GT. Evaluating protein structures determined by structural genomics consortia. Proteins 2007;66:778-95.
34. Huang YJ, Powers R, Montelione GT. Protein NMR recall, precision, and F-measure scores (RPF Scores): Structure quality assessment measures based on information retrieval statistics. J Am Chem Soc 2005;127:1665-74.
35. Laskowski RA, MacArthur MW, Moss DS, Thornton JM. PROCHECK: A program to check the stereochemical quality of protein structures. J Appl Crystallogr 1993;26:283-91.
36. Lovell SC, Davis IW, Arendall WB, de Bakker PIW, Word JM, Prisant MG, *et al.* Structure validation by Cα geometry: ϕ,ψ and Cβ deviation. Proteins 2003;50:437-50.
37. Lüthy R, Bowie JU, Eisenberg D. Assessment of protein models with three-dimensional profiles. Nature 1992;356:83-5.
38. Sippl MJ. Recognition of errors in three-dimensional structures of proteins. Proteins 1993;17:355-62.
39. Trott O, Olson AJ. AutoDock Vina: Improving the speed and accuracy of docking with a new scoring function, efficient optimization, and multithreading. J Comput Chem 2010;31:455-61.
40. Al-Shabib NA, Khan JM, Malik A, Rehman MT, AlAjmi MF, Husain FM, *et al.* Investigating the effect of food additive dye 'tartrazine' on BLG fibrillation under *in-vitro* condition. A biophysical and molecular docking study. J King Saud Univ Sci 2020;32:2034-40.
41. M. Al-Saleem M, Al-Wahaibi L, Rehman M, AlAjmi M, Alkahtani R, Abdel-Mageed W. Phenolic compounds of Heliotropium europaeum and their biological activities. Phcog Mag 2020;16:108-16.
42. Rehman MT, Ahmed S, Khan AU. Interaction of meropenem with 'N' and 'B' isoforms of human serum albumin: A spectroscopic and molecular docking study. J Biomol Struct Dyn 2016;34:1849-64.
43. Rehman MT, Shamsi H, Khan AU. Insight into the binding mechanism of imipenem to human serum albumin by spectroscopic and computational approaches. Mol Pharm 2014;11:1785-97.
44. Kumari R, Kumar R; Open Source Drug Discovery Consortium, Lynn A. g_mmpbsa—a GROMACS tool for high-throughput MM-PBSA calculations. J Chem Inf Model 2014;54:1951-62.
45. Camacho C, Coulouris G, Avagyan V, Ma N, Papadopoulos J, Bealer K, *et al.* Blast+: Architecture and applications. BMC Bioinform 2009;10:421.
46. Steinegger M, Meier M, Mirdita M, Vöhringer H, Haunsberger SJ, Söding J. HH-suite3 for fast remote homology detection and deep protein annotation. BMC Bioinform 2019;20:473.
47. Studer G, Tauriello G, Bienert S, Biasini M, Johner N, Schwede T. ProMod3-A versatile homology modelling toolbox. PLoS Comput Biol 2021;17:e1008667. doi: 10.1371/journal. pcbi. 1008667.
48. Jabir NR, Shakil S, Tabrez S, Khan MS, Rehman MT, Ahmed BA. *In silico* screening of glycogen synthase kinase-3β targeted ligands against acetylcholinesterase and its probable relevance to Alzheimer's disease. J Biomol Struct Dyn 2021;39:5083-92.
49. Mohammad T, Arif K, Alajmi MF, Hussain A, Islam A, Rehman MT, *et al.* Identification of high-affinity inhibitors of pyruvate dehydrogenase kinase-3: Towards therapeutic management of cancer. J Biomol Struct Dyn 2021;39:586-94.
50. King D, Strynadka N. Crystal structure of New Delhi metallo-β-lactamase reveals molecular basis for antibiotic resistance. Protein Sci 2011;20:1484-91.
51. King DT, Worrall LJ, Gruninger R, Strynadka NCJ. New Delhi metallo-β-lactamase: Structural insights into β-lactam recognition and inhibition. J Am Chem Soc 2012;134:11362-5.